Available online at www.sciencedirect.com
ScienceDirect
Materials Chemistry and Physics 108 (2008) 55–60
MATERIALS CHEMISTRY AND PHYSICS
www.elsevier.com/locate/matchemphys

Improving dielectric loss and enhancing figure of merit of $Ba_{0.5}Sr_{0.5}Ti_{0.95}Mg_{0.05}O_3$ thin films doped by aluminum

Shean-Yih Lee [a,*], Bi-Shiou Chiou [a,b], Horng-Hwa Lu [c]

[a] *Department of Electronic Engineering and Institute of Electronics, National Chiao Tung University, Hsin-Chu 300, Taiwan, ROC*
[b] *Innovative Packaging Research Center, National Chiao Tung University, Hsin-Chu 300, Taiwan, ROC*
[c] *Department of Mechanical Engineering, National Chin Yi Technology University, Taiping 411, Taiwain, ROC*

Received 6 March 2007; received in revised form 29 August 2007; accepted 2 September 2007

Abstract

The different Al contents effects of $Ba_{0.5}Sr_{0.5}Ti_{0.95}Mg_{0.05}O_3$ (BSTM) thin films grown on Pt/TiN/SiO_2/Si substrates in the crystallographic structure, surface morphology, dielectric constant, loss tangent, leakage current, and figure of merit were investigated. The BSTM films properties are studied as a function of Al content and have remarkable improvements including dielectric loss, leakage current, and figure of merit (FOM) as well as films grain sizes. With increasing Al content, the dielectric constant (k), tunability (T), loss tangent ($\tan\delta$), and leakage current density (J_L) decrease while the FOM, defined as $T/\tan\delta$, and breakdown strength increases. The maximum dielectric constant at zero bias, tunability, dielectric loss, FOM, and leakage current density of 1 mol% Al-doped BSTM films at 280 kV cm^{-1} are 248, 40%, 0.0093, 43, and 3.76×10^{-7} A cm^{-2}, however, the same measured conditions of undoped BSTM films are 341, 54%, 0.0265, 20, and 1.19×10^{-6} A cm^{-2}, respectively. The dc resistivity increases from 2.33×10^{11} Ω cm of the BSTM film to 6.08×10^{12} Ω cm of the 5 mol% Al-doped BSTM film at 280 kV cm^{-1}. In addition, the tolerance factor (t) of Al-doped BSTM perovskite thin films is 0.97 as compared to 0.87 of the undoped BSTM thin films. The increasing of tolerance factor value indicates that the specimens with Al-doped BSTM films are more stable than undoped specimens.

Keywords: BSTM thin films; Al doped; Grain size; Dielectric loss; Figure of merit (FOM)

1. Introduction

The advancement of dynamic random access memories (DRAMs) has significantly decreased the available area per cell. Electroceramic thin films with high dielectric constant have attracted great attention for practical use in capacitors of gigabit DRAMs since the adoption of high dielectric constant materials can lower the height of the storage node and simplify the cell structure. One of the most promising materials for the capacitor dielectric thin film is the (Ba, Sr)TiO_3 (BST) material [1,2]. Recently, BST thin films are widely investigated for ultra-large scale integrated circuits (ULSIs) DRAM storage capacitors, nonvolatile ferroelectric random access memories (NVFRAM), microelectromechanical systems (MEMS), commercial radio frequency integrated circuits (RFICs), and tunable microwave devices due to these features [3–7]: (1) high dielectric constant, (2) low leakage current, (3) low temperature coefficient of electrical properties, (4) lack of fatigue or aging problems, (5) high compatibility with DRAM device processes, (7) linear relation of electric field and polarization, and (8) low Curie temperature. Hence, the BST thin films are successfully applied in integrated circuit processes. However, an increase of tunability also leads to an increase in the dielectric loss and thereby decreases the figure of merit (FOM) of BST films especially at operating frequencies of tunable/microwave devices [7]. Hence, it is important to decrease the dielectric loss and increase the FOM of BST films in the device fabrication.

According to previous investigations, the electrical and dielectric properties and reliability of BST films heavily depend upon the thin film deposition method, composition, dopant, post-annealed temperature, base electrode, microstructure, film thickness, surface roughness, oxygen content, and homogeneity of the film [1–7]. Kim and Kim [8] reported that the undoped BST thin films are accompanied by high dielectric loss which is much larger than 0.02. Lee and Kim [9] observed that the dielectric properties of thin films are affected by the grain size and

* Corresponding author. Tel.: +886 9 21205813; fax: +886 4 24392556.
E-mail address: yih@ctu.edu.tw (S.-Y. Lee).

0254-0584/$ – see front matter © 2007 Elsevier B.V. All rights reserved.
doi:10.1016/j.matchemphys.2007.09.005

surface roughness of thin films. The dielectric constant as well as the leakage current of BST films decreases with the decrease of grain size and accounts for a smoother surface morphology. Herner and Selmi [10] had improved the dielectric properties by doping foreign ions on the A or B sites of the ABO_3 perovskite structure. These dopants include Mn, Bi, Ga, Y, Nb and Fe. One of the most important researches of these doping materials is Mg-doped $Ba_{0.6}Sr_{0.4}TiO_3$ thin films [11]. Mg ions occupy the B sites of the ($A^{2+}B^{4+}O_3{}^{2-}$) perovskite structure and substitute for Ti ions of BST films. The FOM value of 5 mol% Mg-doped BST films is FOM = 24 [11].

In the present study, we will provide another method to decrease the dielectric loss and enhance the FOM value of $Ba_{0.5}Sr_{0.5}Ti_{0.95}Mg_{0.05}O_3$ (BSTM) films, effectively. The conventional MIM capacitor structure is apt to produce the higher dielectric loss and lower FOM value through manufacturing processes. The doped Al is playing a crucial role during BSTM films crystallization which is employed to improve the BSTM films dielectric and electrical properties including the grain size, surface morphology, dielectric loss, leakage current, and FOM value comparing with the undoped BSTM specimens.

2. Experimental procedures

Planar capacitors were fabricated to investigate the dielectric and electrical properties of the Al-doped BSTM (Ba/Sr = 0.5/0.5) films. The precursor solution of BSTM was prepared by acid-based sol–gel route. Barium acetate $Ba(C_2H_3O_2)_2$ (purity ≥ 99%), strontium acetate $Sr(C_2H_3O_2)_2{\cdot}(1/2)H_2O$ (purity ≥ 99.5%), titanium isopropoxide $C_{12}H_{28}O_4Ti$ (purity ≥ 97%), magnesium acetate $Mg(C_2H_3O_2)_2{\cdot}4H_2O$ (purity ≥ 99.5%), and aluminum acetylacetonate $Al(C_5H_7O_2)_3$ (purity ≥ 99%) were used as starting materials (purchased from Aldrich Chemical Reagent Co., Milwaukee, OR, USA). Glacial acetic acid ($C_2H_4O_2$) and ethylene glycol ($C_2H_6O_2$) were selected as solvents and to reduce the crystallized temperature. Formamide (CH_3NO) was employed to adjust the viscosity of the solution in order to reduce the cracking of Al-doped BSTM films.

The Al concentration of the nominal compositions of BSTM films was added from 0 to 5 mol%. The precursor solution was spin-coated onto a platinized Si wafer (Pt/TiN/SiO_2/Si) by two-step spin-speed processes at a speed of 1500 rpm for 30 s followed by 4000 rpm for 30 s. The stock precursor solution was syringed through a 0.2 μm syringe filter before the thin film deposition. The spun-on precursor solution was dried in air at 150 °C for 10 min and pre-baked at 500 °C for 30 min. The thickness of the baked BSTM films is around 180 nm. A two-step post-annealing process with a furnace annealing in O_2 atmosphere at 700 °C for 1 h followed by an N_2O plasma bombardment at 250 °C for 180 s was then employed. The purpose of the N_2O plasma treatment is to reduce the carbon contaminants, such as CH_4, CO, and CO_2 molecules, which act as the electron traps near the surface of BSTM films. Structure characteristics of the annealed Al-doped BSTM thin films were exactly analyzed by a grazing incident X-ray diffractometer (GIXRD, Philips, X'pert Pro MRD) with Cu Kα radiation (wavelength, λ ~ 1.5428 Å) at 45 kV, 40 mA. The surface morphologies of thin films were observed via atomic force microscopy (AFM, Digital Instruments Nano-Scope III).

The measurements of dielectric properties of Al-doped BSTM films were carried out using the metal–insulator–metal (MIM) capacitor configuration. The leakage current density versus electric field (J_L–E) measurement was performed using a semiconductor parameter analyzer (HP 4156, Hewlett-Packard Co., USA). The capacitance–voltage (C–V) characteristics were measured with a precision LCR meter (HP 4284, Hewlett-Packard Co., USA) in the frequency range of 20 Hz–1 MHz. The Pt top electrode of Al-doped BSTM capacitors was connected to the voltage source and the bottom electrode was grounded. The cross-sectional structure of the capacitor is illustrated in Fig. 1. The top and bottom Pt electrodes were deposited by dc sputtering.

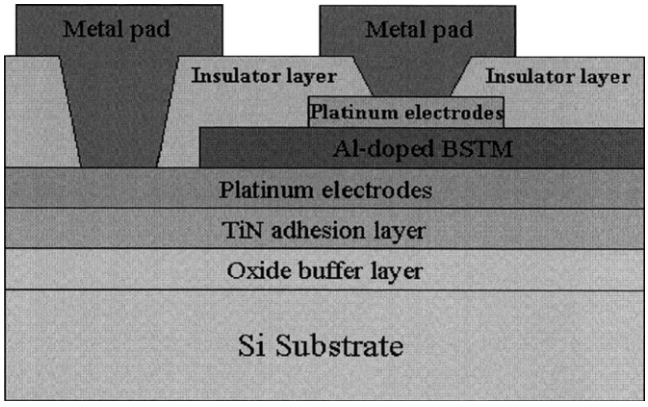

Fig. 1. Schematic cross-section of Al-doped BSTM film capacitor structure in this study.

3. Results and discussion

Fig. 2 shows the grazing incident X-ray diffraction patterns of BSTM thin films as a function of Al concentration. The crystal structure is BSTM phase and without second phase. The XRD results suggest that the dopants have entered the unit-cell maintaining the perovskite structure of the solid solution. According to the Scherrer formula, the average grain size can be estimated by

$$D = \frac{0.9\lambda}{B\cos\theta} \quad (1)$$

where D is the grain size, λ the X-ray wavelength (λ ~1.5428 Å), B the full-width at half-maximum (FWHM) of the XRD peak, and θ is the diffraction angle. The grain sizes of Al-doped BSTM films with the (1 1 0) peak in the XRD patterns are listed in Table 1. The grain sizes of the undoped, 1, 3, and 5 mol% Al-doped BSTM samples are 14.1, 13.6, 13.0, and 12.6 nm, respectively. The result suggests that the grain size decreases with the increasing of Al concentration.

The typical AFM images of Al-doped BSTM films were shown in Fig. 3. The measurement of root-mean-square surface roughness (R_{rms}) of Al-doped BSTM films is 3.855 (undoped), 3.635 (1 mol% Al-doped), 3.324 (3 mol% Al-doped), and

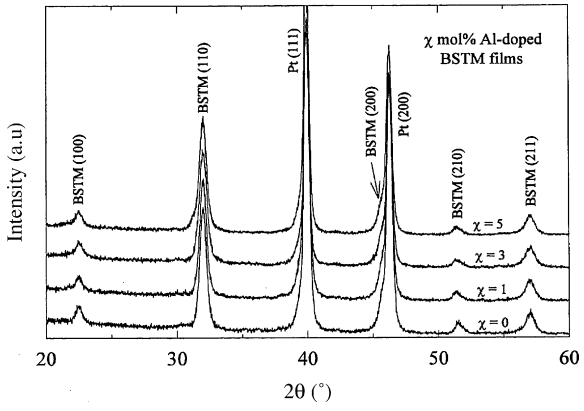

Fig. 2. Grazing incident X-ray diffraction patterns (GIXRD) of undoped, 1, 3, and 5 mol% Al-doped BSTM films deposited on Pt/TiN/SiO_2/Si.

Table 1
Grain size, maximum dielectric constant (k_{max}) at zero bias and 100 kHz, maximum tunability (T_{max}), loss tangent ($\tan\delta$), leakage current density (J_L), and figure of merit (FOM) of χ mol% Al-doped BSTM films are measured at 280 kV cm^{-1}

χ	Grain size (nm)	k_{max}	T_{max} (%)	$\tan\delta$	J_L (μA cm^{-2})	FOM
0	14.1	341	54	0.0265	1.192	20
1	13.6	248	40	0.0093	0.376	43
3	13.0	170	25	0.0085	0.148	29
5	12.6	106	9	0.0071	0.046	13

3.048 nm (5 mol% Al-doped), respectively. It is indicated that the surface roughness decreases with increasing Al-doped concentration. According to the Cukauskas's investigation [12], the amorphous or a small grain size film usually had a smoother surface. The Al dopant appears to suppress grain growth accounted for the grain size decreases. The Al-doped BSTM film with a small grain size exhibits a smoother surface morphology which accounts for a lower dielectric loss. This trend is consistent with that previously reported [9]. Consequently, the improvement of dielectric and leakage characteristics could be achieved through the improvement of surface roughness, variation of grain size and/or compensation of oxygen vacancies near the surface [13].

The tolerance factor (t) has been used to evaluate the stability of the perovskite (ABO_3) type compounds and is defined as [14]:

$$t = \frac{r_A + r_O}{\sqrt{2}(r_B + r_O)} \quad (2)$$

where r_A, r_B and r_O represent the ionic radius of ions occupying A-site, B-site and oxygen ion, respectively. If $t > 1.0$, the space available for the B-site ion in the lattice is larger than that of A-site ion, and if $t < 1.0$, the space available for the A-site ion is larger than that of B-site ion. The perovskite structure is known to be stable only for $0.9 \leq t \leq 1.1$ [14]. On the basis of ionic radii for Mg^{2+} ($r_{eff} = 0.72$ Å), Ti^{4+} ($r_{eff} = 0.61$ Å), and Al^{3+} ($r_{eff} = 0.53$ Å) in the sixfold coordination, it is assumed that Mg or Al replaces Ti sites in the Al-doped BSTM lattice. According to Eq. (2), the tolerance factor for Mg ions residing at Ti sites is 0.87 which is smaller than Al ions residing at Ti sites ($t = 0.97$). It suggests that Al-doped BSTM films are more stable than undoped BSTM specimens.

The leakage current density versus applied electric field (J_L–E) for Al-doped BSTM films at room temperature is shown in Fig. 4. The Al-doped BSTM films on Pt/TiN/SiO_2/Si(1 0 0) substrates exhibit good insulating properties, the leakage current density of the 5 mol% Al-doped BST film ($J_L = 4.62 \times 10^{-8}$ A cm^{-2}) is about 2 order of magnitude lower than that of the undoped BSTM film ($J_L = 1.19 \times 10^{-6}$ A cm^{-2}) at 280 kV cm^{-1}. The leakage current can be affected by the surface roughness and grain sizes. The smaller grain size produces more grain boundaries, therefore, the films with higher breakdown field and lower leakage current density can be obtained [15]. Hence, it is suggested that the decrease of the leakage current of Al-doped BSTM specimens can be attributed to the reduction of the surface roughness.

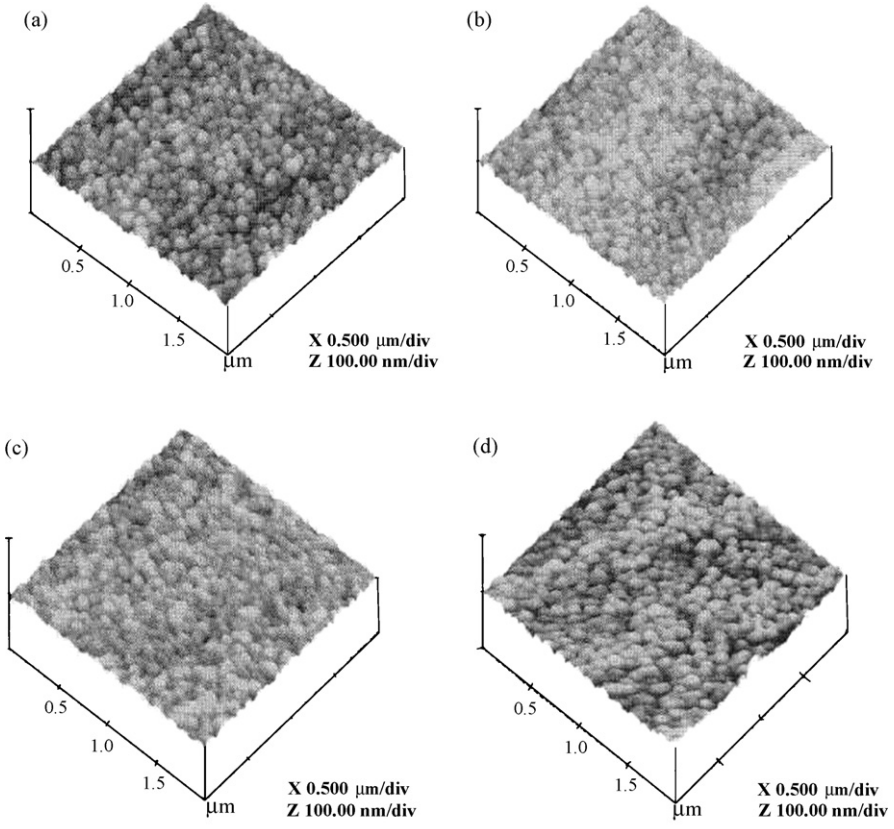

Fig. 3. AFM images of (a) undoped, (b) 1 mol%, (c) 3 mol%, and (d) 5 mol% Al-doped BSTM thin films.

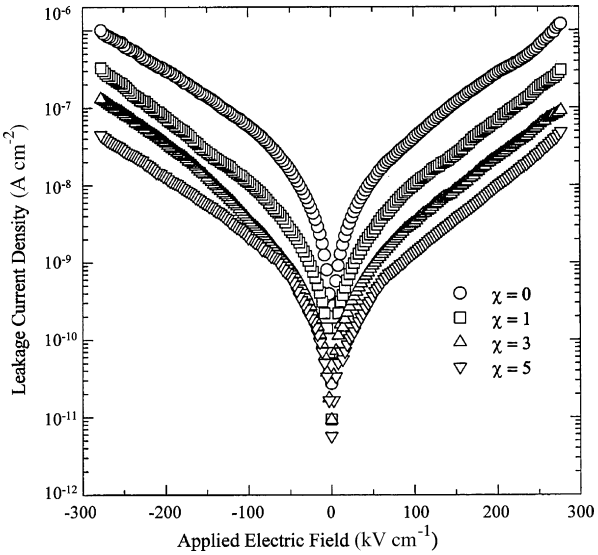

Fig. 4. The leakage current density vs. applied electric field of χ mol% Al-doped BSTM films at room temperature.

The dc resistivity of Al-doped BSTM films varies from $2.33 \times 10^{11}\ \Omega$ cm (undoped) to $6.08 \times 10^{12}\ \Omega$ cm (5 mol% Al-doped) at 280 kV cm^{-1}. It is suggested that inherent grain boundary donor-type interface states such as immobile Ti^{4+} or Ti^{3+} interstitial ions and mobile $V_O^{\bullet\bullet}$ or holes were eliminated by negative space charges [16]. The formations of negative space charge regions should reduce the local conductivity at grain boundaries and hence reduce the leakage current density in Al-doped BSTM films. Besides, the Al doping enhances the insulation resistance of BSTM films by suppressing the concentration of oxygen vacancies and increasing the potential barrier at grain boundaries.

Fig. 5 shows the dielectric constant (k) and loss tangent ($\tan\delta$) at room temperature as a function of applied electric field at 100 kHz. The maximum dielectric constant and loss tangent (k_{max}, $\tan\delta$) at zero bias voltage of undoped, 1, 3, and 5 mol% Al-doped BSTM samples are (341, 0.0465), (248, 0.0108), (170, 0.0093), and (106, 0.0076), respectively. The reasons that Al-doped BSTM films have smaller dielectric loss are: (a) the Al^{3+} ion attracts and neutralizes jumping electrons between the different titanium ions which provides a mechanism for dielectric losses and leads to the dielectric loss reduced, and (b) Al^{3+} ions occupy the B sites of Ti^{4+} in the ABO_3 perovskite structure and behave as electron acceptor-like dopants. These acceptors prevent the reduction of Ti^{4+} to Ti^{3+} by neutralizing the donor action of the oxygen vacancies which can be polarized under an alternating electric field [17]. Besides, high temperature annealing in the air atmosphere (i.e., a slightly reducing ambience) creates intrinsic oxygen vacancies in BSTM films. Lee and Tseng [18] illustrates that a dopant ion carries the extra negative charges and compensates the positive charges of the oxygen vacancies, as a result the concentration of free carriers (electrons) is reduced. The decrease in electron concentration leads to lower leakage current and dielectric loss as compared to the undoped specimens. On the other hand, the different ionic radii ratio between Al^{3+} and Ti^{4+} is 13%, but the ratio between Al^{3+} and Mg^{2+} is

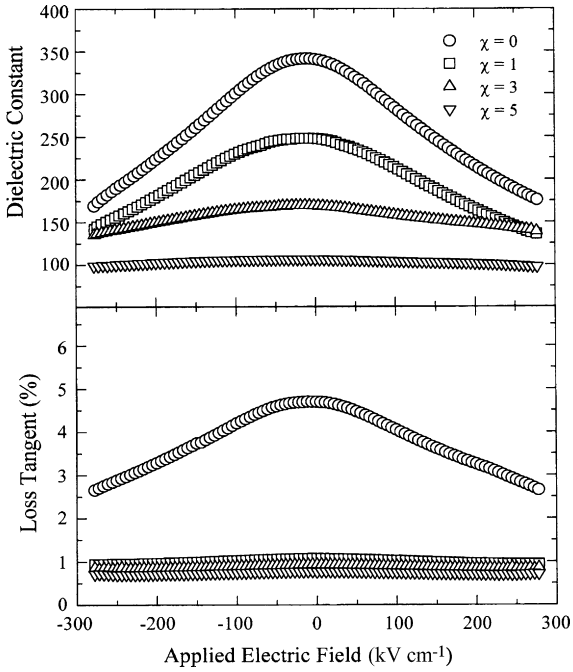

Fig. 5. Dielectric constant and loss tangent of χ mol% Al-doped BSTM thin films as a function of applied electric field at 100 kHz.

26% in Al-doped BSTM films. Besides, the electronegativity of Al, Mg and Ti atom is 1.5, 1.2, and 1.5, respectively. It suggests that the Al ion has a similar ionic radii and same electronegativity to Ti ions. But, the ionic radii and electronegativity are largely different between Al and Mg ions. Hence, the Al ions are less probable to occupy Mg sites in BSTM films.

The dielectric constant (k) and loss tangent ($\tan\delta$) of BSTM films at room temperature as a function of measured frequency (f) is shown in Fig. 6. The undoped BSTM film has the high-

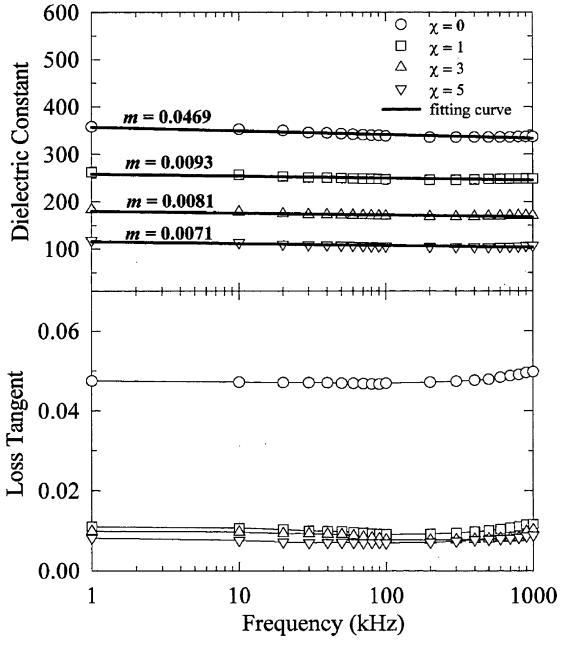

Fig. 6. Dielectric constant and loss tangent as a function of measured frequency for χ mol% Al-doped BSTM films. The curves are fitted with $k = k_{1\,kHz} f^{-m}$.

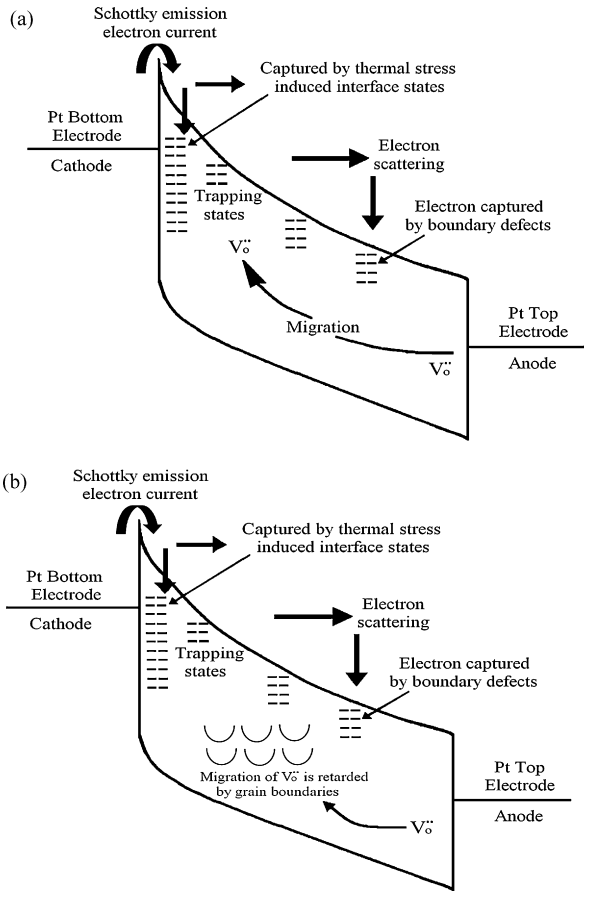

Fig. 7. Schematic diagram for the conduction mechanism of (a) undoped BSTM films and (b) Al-doped BSTM films.

est dielectric constant and the dielectric constant decreases with increasing Al content. In Fig. 6, a power law dependence of dielectric constant (k) on frequency (f) is observed, that is, $k = k_{1\,\mathrm{kHz}} f^{-m}$, where $k_{1\,\mathrm{kHz}}$ is the dielectric constant at 1 kHz and the power m is the dispersion parameter. The different power m value in the power-law relationship in dielectric dispersion can be simply estimated by way of the curve fitting of dielectric constant versus frequency curve. The dispersion parameter m decreases with the increase of Al concentration as indicated in Fig. 6. The m value obtained from curve fitting of undoped, 1, 3, and 5 mol% Al-doped BSTM thin films is 0.0469, 0.0093, 0.0081, and 0.0071, respectively. According to Balu's investigations [19], the dielectric loss may be caused by interactions between the dielectric material and the up/bottom electrode during thin film deposition and/or due to poor film quality during the initial stages of deposition. Hence, these results suggested that the fabrication process, dopant, the quality of interface and bulk could affect the power m value in Al-doped BSTM films.

The conduction mechanism of Al-doped BSTM films is proposed and schematically shown in Fig. 7. There is residual thermal stress existed in the annealed BSTM/Pt film, this stress induces interface states as exhibited in Fig. 7(a). Generally, the scattering of charge carriers, the charge carrier detrapping rate and the migration of oxygen vacancies govern the leakage current. Besides, Hwang et al. [20] reported that contacts between Pt electrode and perovskite oxide thin films had Schottky-type characteristics due to the surface adsorptions and/or broken bonds on the surface. Hence, under a relatively high field, the migration and pilling of intrinsic oxygen vacancies near the cathode would lower the resistance of the Schottky junction and result in a larger leakage current [21]. For the Al-doped BSTM films, there are more grain boundary areas due to the smaller grain sizes which are considered that the grain boundary in dielectric ceramics represents a resistance and the grain boundaries would retard the migration of oxygen vacancy, as exhibited in Fig. 7(b).

The tunability (T) is defined as $(k_{\max} - k_v)/k_{\max}$, where $k_{\max}$ and k_v represent the maximum dielectric constant at zero bias and a certain electric field, respectively. The tunable characteristic of Al-doped BSTM films as a function of applied electric field is shown in Fig. 8. The tunability decreases with increasing Al content from $T = 54\%$ (undoped) to $T = 9\%$ (5 mol% Al-doped) measured at 280 kV cm^{-1} and the tunability variation is also listed in Table 1. The decrease in dielectric constant and tunability is attributed to the decrease in grain size and crystallinity of the Al-doped BSTM films. The decrease in grain size not only decreases the volume of polarization but also increases the amount of low dielectric constant grain boundaries and/or induces more grain boundary defects per unit volume.

Fig. 9 shows the variation of FOM as a function of applied electric field. The FOM is frequently used as a parameter to characterize correlations between tunability and loss tangent. This parameter is defined as FOM = tunability/tan δ. The FOM value reflects the fact that a tunable microwave circuit cannot take full advantages of high tunability if the dielectric loss is too high. Practically, the FOM value should be as high as possible for a design criterion of tunable microwave devices. The highest FOM value is obtained of the 1 mol% Al-doped BSTM films (FOM = 43) as compared with undoped BSTM specimens (FOM = 20).

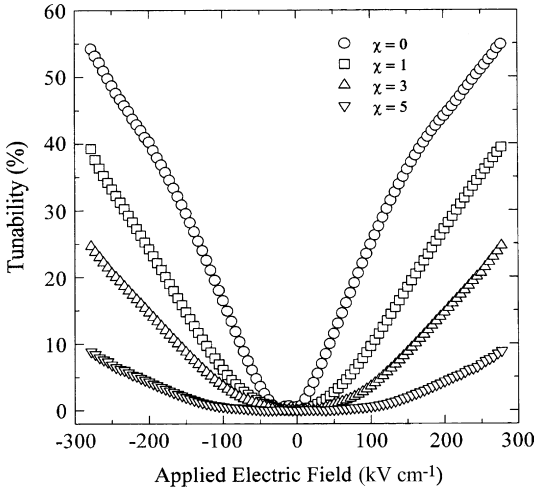

Fig. 8. Tunability as a function of applied electric field at 100 kHz of χ mol% Al-doped BSTM thin films.

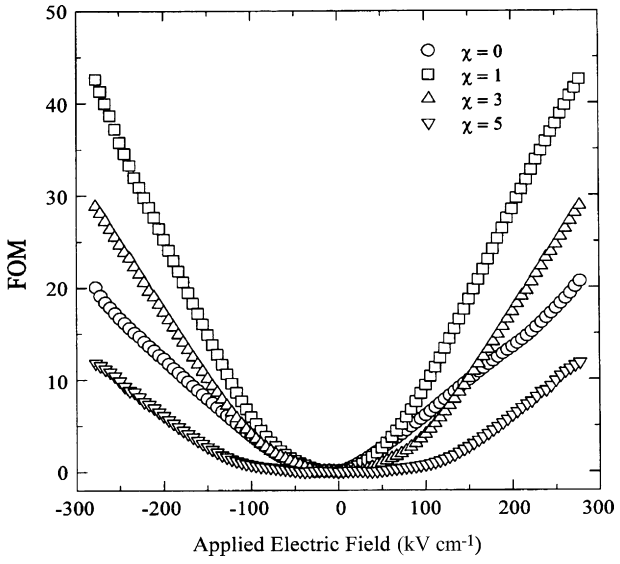

Fig. 9. FOM as a function of applied electric field of χ mol% Al-doped BSTM films measured at 100 kHz.

4. Conclusions

Microstructure, dielectric and electrical properties of Al-doped BSTM thin films have been investigated by sol–gel spin coating process. The Al dopant decreases the grain size and surface roughness of BSTM films. The maximum dielectric constant (k) at zero bias and loss tangent ($\tan\delta$) at 280 kV cm^{-1} is 341 (k) and 0.0265 ($\tan\delta$) of the undoped BSTM films as compared with those of 106 (k) and 0.0071 ($\tan\delta$) of the 5 mol% Al-doped BSTM specimens. The decrease of dielectric constant and dielectric loss with increasing the Al-doped concentration is associated with the decrease in grain size of the thin film, because the volume of polarization is less for films with small grains as compared with undoped films with large grains. Hence, the Al-doped BSTM films result in a lower dielectric constant, tunability, dielectric loss and leakage current. However, the maximum FOM value is obtained from 1 mol% Al-doped BSTM films (FOM = 43) compared with undoped BSTM films (FOM = 20). The result indicates that Al-doped BSTM films can effectively decrease the dielectric loss and promote the figure of merit characteristics for the applications of MIM capacitor constructions.

Acknowledgement

The authors gratefully appreciate financial support from the National Science Council of the Republic of China under Project no. NSC 95-2221-E-009-085.

References

[1] J.W. Liou, B.S. Chiou, Mater. Chem. Phys. 51 (1997) 59.
[2] S. Ezhilvalavan, T.Y. Tseng, Mater. Chem. Phys. 65 (2000) 227.
[3] Y.R. Liu, P.T. Lai, G.Q. Li, B. Li, J.B. Peng, H.B. Lo, Mater. Chem. Phys. 94 (2005) 114.
[4] Y.J. Seo, W.S. Lee, Microelectron. Eng. 75 (2004) 149.
[5] Z. Wang, J. Liu, T. Ren, L. Liu, Sens. Actuators A 117 (2005) 293.
[6] Y. Tsunemine, T. Okudaira, K. Kashihara, A. Yutani, H. Shinkawata, M.K. Mazumder, Y. Ohno, M. Yoneda, Y. Okuno, A. Tsuzumitani, H. Ogawa, Y. Mori, Jpn. J. Appl. Phys. 43 (2004) 2457.
[7] R.H. Liang, X.L. Dong, Y. Chen, F. Cao, Y.L. Wang, Mater. Chem. Phys. 95 (2006) 222.
[8] K.T. Kim, C.I. Kim, Surf. Coat. Technol. 200 (2006) 4708.
[9] W.J. Lee, H.G. Kim, J. Appl. Phys. 80 (1996) 5891.
[10] S.B. Herner, F.A. Selmi, V.V. Varadan, V.K. Varadan, Mater. Lett. 15 (1993) 317.
[11] M.W. Cole, P.C. Joshi, M.H. Ervin, M.C. Wood, R.L. Pfeffer, Thin Solid Films 374 (2000) 34.
[12] E.J. Cukauskas, S.W. Kirchoefer, J.M. Pond, J. Appl. Phys. 88 (2000) 2830.
[13] D.C. Shye, C.C. Hwang, C.C. Jaing, H.W. Hsu, J.S. Chen, B.S. Chiou, H.C. Cheng, Jpn. J. Appl. Phys. 42 (2003) 549.
[14] S. Shirasaki, H. Yamamura, H. Haneda, J. Chem. Phys. 73 (1980) 4640.
[15] M.S. Tsai, S.C. Sun, T.Y. Tseng, J. Appl. Phys. 82 (1997) 3428.
[16] Y.M. Ching, T. Takagi, J. Am. Ceram. Soc. 73 (1990) 3278.
[17] X. Liang, W. Wu, Z. Meng, Mater. Sci. Eng. B 99 (2003) 366.
[18] S.Y. Lee, T.Y. Tseng, Appl. Phys. Lett. 80 (2002) 1797.
[19] V. Balu, T.S. Chen, S. Katakam, J.H. Lee, B. White, S. Zafar, B. Jiang, P. Zurcher, R.E. Jones, J. Lee, Integr. Ferroelectr. 21 (1998) 155.
[20] C.S. Hwang, S.O. Park, C.S. Kang, H.J. Cho, H.K. Kang, S.T. Ahn, M.Y. Lee, Jpn. J. Appl. Phys. 34 (1995) 5178.
[21] M.S. Tsai, T.Y. Tseng, Mater. Chem. Phys. 57 (1998) 47.